frontiers in Physics

MINI REVIEW
published: 02 February 2022
doi: 10.3389/fphy.2021.813532

Low Valence Nickelates: Launching the Nickel Age of Superconductivity

Antia S. Botana[1], Kwan-Woo Lee[2], Michael R. Norman[3], Victor Pardo[4,5] and Warren E. Pickett[6]*

[1]Department of Physics, Arizona State University, Tempe, AZ, United States, [2]Division of Display and Semiconductor Physics, Korea University, Sejong, South Korea, [3]Materials Science Division, Argonne National Laboratory, Lemont, IL, United States, [4]Departamento de Física Aplicada, Facultade de Física, Universidade de Santiago de Compostela, Santiago de Compostela, Spain, [5]Instituto de Materiais (iMATUS), Universidade de Santiago de Compostela, Santiago de Compostela, Spain, [6]Department of Physics and Astronomy, University of California, Davis, Davis, CA, United States

The discovery of superconductivity in thin films (~10 nm) of infinite-layer hole-doped $NdNiO_2$ has invigorated the field of high temperature superconductivity research, reviving the debate over contrasting views that nickelates that are isostructural with cuprates are either 1) sisters of the high temperature superconductors, or 2) that differences between nickel and copper at equal band filling should be the focus of attention. Each viewpoint has its merits, and each has its limitations, suggesting that such a simple picture must be superseded by a more holistic comparison of the two classes. Several recent studies have begun this generalization, raising a number of questions without suggesting any consensus. In this paper, we organize the findings of the electronic structures of n-layered NiO_2 materials (n = 1 to ∞) to outline (ir) regularities and to make comparisons with cuprates, with the hope that important directions of future research will emerge.

Keywords: superconductivity, electronic structure ab-initio calculations, nickelates, magnetism, cuprates electronic structure

Edited by:
Matthias Eschrig, University of Greifswald, Germany

Reviewed by:
Andrzej M. Oles, Jagiellonian University, Poland

****Correspondence:***
Antia S. Botana
antia.botana@asu.edu

Specialty section:
This article was submitted to Condensed Matter Physics, a section of the journal Frontiers in Physics

Received: *11 November 2021*
Accepted: *14 December 2021*
Published: *02 February 2022*

Citation:
Botana AS, Lee K-W, Norman MR, Pardo V and Pickett WE (2022) Low Valence Nickelates: Launching the Nickel Age of Superconductivity. Front. Phys. 9:813532. doi: 10.3389/fphy.2021.813532

1 BACKGROUND

After much synthesis and characterization of low-valence layered nickelates over three decades [1–7], superconductivity was finally observed [8] in hole-doped $\mathcal{R}NiO_2$ (initially for rare earth $\mathcal{R}$ = Nd, later for $\mathcal{R}$ = La [9, 10] and Pr [11]) with T_c exhibiting a dome-like dependence [12, 13] being maximal (10–15 K) near 20% doping. This series of discoveries in $\mathcal{R}NiO_2$ materials marked the beginning of a new, nickel age of superconductivity [14, 15] launching a plethora of experimental [16–22] and theoretical [23–43] work.

$\mathcal{R}NiO_2$ materials are the $n = \infty$ member of a larger series of layered nickelates with chemical formula $(\mathcal{R}O_2)^-[\mathcal{R}(NiO_2)_n]^+$ ($\mathcal{R}$ = La, Pr, and Nd; $n = 2, 3, \ldots, \infty$) that possess n cuprate-like NiO_2 planes in a square-planar coordination. Except for the $n = \infty$ case, groups of n-NiO_2 layers are separated by $\mathcal{R}_2O_2$ blocking layers that severely limit coupling between adjacent units (see **Figure 1**). These layered square-planar compounds are obtained via oxygen deintercalation from the corresponding parent perovskite $\mathcal{R}NiO_3$ ($n = \infty$) [2] and Ruddlesden-Popper $\mathcal{R}_{n+1}Ni_nO_{3n+1}$ ($n \neq \infty$) phases [1]. As shown in **Figure 1**, the $(\mathcal{R}O_2)^-[(\mathcal{R}NiO_2)_n]^+$ series can be mapped onto the cuprate phase diagram in terms of the nickel $3d$-electron count, with nominal fillings running from d^9 ($n = \infty$) to d^8 (for n = 1). That superconductivity arises in this series suggests that a new family of superconductors has been uncovered, currently with two members, $n = \infty$ and n = 5 [44], the only ones (so far) where an optimal Ni valence near $d^{8.8}$ has been attained.

Some overviews on experimental and theoretical findings in this family of materials have been recently published [45–48]. In this paper, we focus on the electronic structure of layered nickelates,

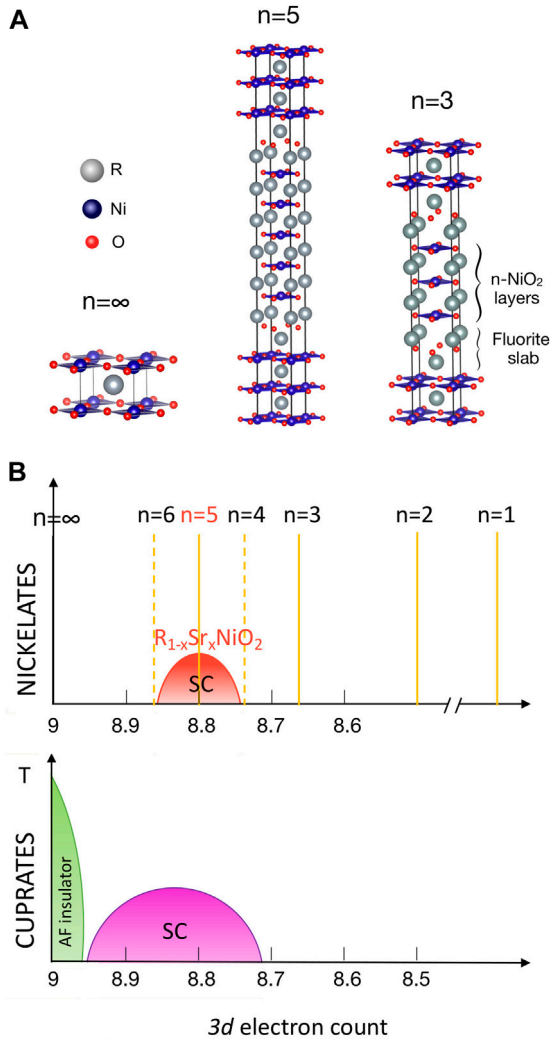

FIGURE 1 | (A) Crystal structures of the $n = \infty$, $n = 5$, and $n = 3$ layered nickelates highlighting the presence of the n-NiO_2 layers and the fluorite blocking slabs present in the $n \neq \infty$ materials. $\mathcal{R}$, Ni and O atoms are shown in gray, blue, and red, respectively. **(B)** Schematic phase diagram as a function of nominal d filling for layered nickelates (top) and cuprates (bottom), highlighting the regions where superconducting domes have been experimentally reported. The members of the $\mathcal{R}_{n+1}Ni_nO_{2n+2}$ series are marked with lines (dashed lines correspond to materials that have not been synthesized yet). The $n = 5$ member falls close to the optimal doping value for both cuprates and the infinite-layer nickelate.

confining ourselves to materials with the basic infinite-layer structure: n square planar NiO_2 layers each separated by an $\mathcal{R}^{3+}$ ion without the apical oxygen ion(s) that are common in most cuprates and nickelates.

2 FROM ∞ TO ONE

2.1 "Infinite-Layer" $n = \infty$ Nickelate: $\mathcal{R}NiO_2$

In parent $\mathcal{R}NiO_2$ materials, Ni has the same formal $3d^9$ electronic configuration as in cuprates. As mentioned above, superconductivity in $\mathcal{R}NiO_2$ materials emerges via hole doping, with T_c exhibiting a dome-like dependence [12, 13, 49] akin to cuprates, as shown in **Figure 1**. However, in parent infinite-layer nickelates the resistivity shows a metallic T-dependence (but with a low temperature upturn) [7, 8] and there is no signature of long-range magnetic order, even though the presence of strong antiferromagnetic (AFM) correlations has recently been reported via resonant inelastic x-ray scattering (RIXS) experiments [50]. This is in contrast to cuprates, where the parent phase is an AFM charge-transfer insulator.

Noteworthy differences from cuprates were already reflected in early electronic structure calculations as well [51, 52]. For the parent material $\mathcal{R}NiO_2$, non-magnetic density functional theory (DFT) calculations show that besides the Ni-$d_{x^2-y^2}$ band, additional bands of $\mathcal{R}$-5d character cross the Fermi level. The electronic structure of $\mathcal{R}NiO_2$ is three-dimensional-like, with a large c-axis dispersion of both (occupied) Ni and (nearly empty) $\mathcal{R}$-5d_{z^2} bands (see **Figure 2**) due to the close spacing of successive NiO_2 planes along the c-axis. The $\mathcal{R}$-5d_{z^2} dispersion leads to the appearance of electron pockets at the Γ and A points of the Brillouin zone which display mainly $\mathcal{R}$-5d_{z^2} and $\mathcal{R}$-5d_{xy} character, respectively, that self-dope the large hole-like Ni-$d_{x^2-y^2}$ Fermi surface. This self-doping effect (absent in the cuprates) introduces a substantial difference between nominal and actual filling of the Ni-d bands, accounting for conduction and possibly also disrupting AFM order. The presence of the 5d electrons is consistent with experimental data, which reveal not only metallic behavior but also evidence for negative charge carriers as reflected in the negative Hall coefficient [8, 12, and 13]. However, as the material becomes doped with Sr, the $\mathcal{R}$-5d pockets become depopulated, the Hall coefficient changes sign [8], and the electronic structure becomes more single-band, cuprate-like [39, 53].

Besides the presence of $\mathcal{R}$-5d electrons, infinite-layer nickelates have some other relevant differences from the cuprates, particularly their much larger charge-transfer energy between the metal 3d, and oxygen 2p states. In cuprates, the charge-transfer energy ε_{3d}-ε_{2p} is as small as 1–2 eV [54], indicative of a large p-d hybridization, and enabling Zhang-Rice singlet formation. In $NdNiO_2$, the charge-transfer energy is much larger, ~4.4 eV, as obtained from the on-site energies derived from a Wannier analysis [39]. The lack of a pre-peak in x-ray absorption (XAS) data at the oxygen K-edge [18] in $NdNiO_2$ has indeed been associated to the presence of a large charge-transfer energy. Because of this increase in charge transfer energy, the nickelate is more Mott-like, whereas the cuprate is more charge-transfer-like, in the scheme of Zaanen, Sawatzky, and Allen [35, 38]. In addition, theoretical investigations of $\mathcal{R}NiO_2$ find decreasing oxygen content as one traverses from La to Lu [55].

The doped holes tend to be on the Ni sites, as opposed to cuprates where they tend to reside on the oxygen sites. Recent DFT + DMFT Ni $2p_{3/2}$ core-level XPS, XAS, and RIXS calculations (consistent with available core-level spectroscopies) indeed confirm that the Ni-O hybridization does not play an important role in connection with doping, implying that the physics of $NdNiO_2$ is well described by a single-band Hubbard model [56]. This in turn brings up the issue of the nature of the doped holes on the Ni sites. That is, do

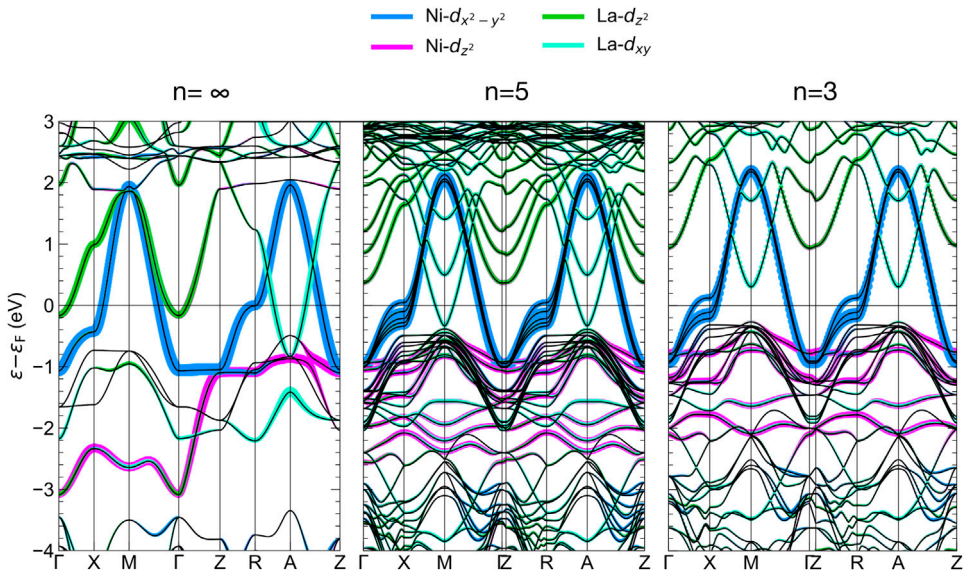

FIGURE 2 | DFT band structures in the paramagnetic state for the $n = \infty$, $n = 5$, and $n = 3$ layered nickelates. The two types of Ni e_g bands are highlighted, as well as the two relevant $\mathcal{R}$-5*d* bands (La is used as an example). It can be observed how the involvement of $\mathcal{R}$-d bands around the Fermi level is reduced with decreasing *n*.

they behave as effective d^8 dopants, and if so, is d^8 high-spin (S = 1) or low-spin (S = 0)? If the former, then these materials would fall in the category of Hund's metals, and thus would deviate substantially from cuprates. DMFT calculations are consistent with this picture as they systematically favor high-spin d^8 (S = 1) states [40, 57–60]. DFT calculations point instead towards a cuprate-like low-spin (S = 0) picture due to the large crystal-field splitting of the e_g states in a square planar environment [53]. Along these lines, impurity calculations show that in the NiO_2 layers a Zhang-Rice singlet (like in CuO_2) is indeed favored upon hole-doping [35]. Further, cluster calculations find that hole doping distributes over the entire cluster, in contrast to local S = 1 states [61].

Because of their lower degree of $p - d$ hybridization, the superexchange in $\mathcal{R}NiO_2$, as determined by resonant inelastic x-ray scattering experiments [50], is about half that of the cuprates. Still, its value (J = 64 meV) confirms the existence of significant AFM correlations [30, 50]. Long-range AFM order has however not been reported, with NMR data suggesting the ground state is paramagnetic [62], and susceptibility data interpreted as spin-glass behavior [63]. Neél type order is consistently obtained in DFT studies [24, 27, 29, and 51], as in d^9 insulating cuprates. The predicted AFM ground state in DFT + U calculations [64] is characterized by the involvement of both $d_{x^2-y^2}$ and d_{z^2} Ni bands [65]. This state is peculiar in that it displays a flat-band one-dimensional-like van Hove singularity of d_{z^2} character pinned at the Fermi level. These flat-band instabilities should inhibit but not eliminate incipient AFM tendencies [65].

Discussing the origin of superconductivity in $\mathcal{R}NiO_2$, as in the cuprates, is a controversial topic. But certainly the reduced T_c of the nickelate compared to the cuprates is consistent with the reduced value of the superexchange, and the larger charge-transfer energy. *t-J* model and RPA calculations building from tight-binding parameters derived from DFT calculations show that the dominant pairing instability is in the $d_{x^2-y^2}$ channel, as in cuprates [66]. Indeed, single-particle tunneling measurements on the superconducting infinite-layer nickelate have revealed a V-shape feature indicative of a *d*-wave gap [67]. On a broader level, several theoretical papers have speculated that the superconductivity is instead an interfacial effect of the infinite-layer film with the $SrTiO_3$ substrate [68–71], though recently superconductivity has been observed when other substrates are used [72]. In this context, it should be noted that superconductivity has not been observed in bulk samples yet; since the precursor is cubic, there is no set orientation for the *c*-axis, meaning the bulk is far less ordered than the film [20, 21].

2.2 The Superconducting $n = 5$ Material

Recently, a second superconducting member has been found in the $(\mathcal{R}O_2)^-[(\mathcal{R}NiO_2)_n]^+$ family: the $n = 5$ layered nickelate $Nd_6Ni_5O_{12}$, also synthesized in thin-film form [44]. As schematically shown in **Figure 1**, this material has a nominal valence near that of the optimally-doped infinite-layer material (that is, $Ni^{1.2+}$: $d^{8.8}$ nominal filling) and so, in contrast to its infinite-layer counterpart, it is superconducting without the need for chemical doping. While $\mathcal{R}NiO_2$ displays NiO_2 layers separated by $\mathcal{R}$ ions, this quintuple-layer material (with five NiO_2 layers per formula unit) has an additional fluorite $\mathcal{R}_2O_2$ slab separating successive five-layer units. Further, each successive five-layer group is displaced by half a lattice constant along the *a* and *b* directions (i.e., the body centered translation of the *I*4/*mmm* space group). These additional structural features effectively decouple the five-layer blocks, so the *c*-axis dispersion of this material is much weaker than its infinite-layer counterpart. Despite these significant structural

differences, T_c is similar to that of the doped infinite-layer materials (with the onset of the superconducting transition taking place at ~ 15 K), reducing the chances that yet to be synthesized low valence nickelates will have substantially higher transition temperatures.

In terms of its electronic structure [73], the $n = 5$ material is intermediate between cuprate-like and $n = \infty$-like behavior. From DFT calculations, the charge-transfer energy of $Nd_6Ni_5O_{12}$ is ~ 4.0 eV. This reduced energy compared to the undoped infinite-layer material means that the Ni-3*d* states are not as close in energy to the Nd-5*d* states, consistent with the presence of a pre-peak in the oxygen K-edge (similar to what happens with Sr-doped $NdNiO_2$ [53]). As a consequence, the electron pockets arising from the Nd-5*d* states are significantly smaller than those in the infinite-layer material (see **Figure 2**). This reduced pocket size along with the large hole-like contribution from the Ni-3*d* states is consistent with experiment in that the Hall coefficient remains positive at all temperatures, with a semiconductor-like temperature dependence reminiscent of under- and optimally-doped layered cuprates. Aside from the appearance of these small Nd-derived pockets at the zone corners, the Fermi surface of $Nd_6Ni_5O_{12}$ is analogous to that of multilayer cuprates with one electron-like and four hole-like $d_{x^2-y^2}$ Fermi surface sheets. Importantly, the Fermi surface of the quintuple-layer nickelate is much more two-dimensional-like compared to the infinite-layer nickelate material, as the presence of the fluorite blocking slab reduces the *c*-axis dispersion, as mentioned above.

2.3 The $n = 3$ Material, the Next Superconducting Member of the Series?

The materials discussed above can be put into the context of earlier studies of bulk reduced RP phases with $n = 2, 3$ NiO_2 layers [5, 74–76], separated by fluorite $\mathcal{R}_2O_2$ blocking slabs that enforce quasi-2D electronic and magnetic behavior.

The $n = 3$ member of the series, $\mathcal{R}_4Ni_3O_8$ (with $Ni^{1.33+}$: $d^{8.67}$ filling), has been studied extensively over the past decade (both single crystal and polycrystralline samples) [74]. Since the charge-transfer energy decreases with decreasing n [73], the $n = 3$ class is more cuprate-like than its $n = \infty$ and $n = 5$ counterparts. Both La and Pr materials are rather similar regarding their high-energy physics, with a large orbital polarization of the Ni-e_g states, so that the d^8 admixture is low spin [75, 77] (but see Ref. [78]). The primary difference is that $La_4Ni_3O_8$ exhibits long-range stripe order [76, 79] (similar to that seen in 1/3 hole-doped La_2NiO_4), consisting of diagonal rows of Ni^{1+} (S = 1/2) and Ni^{2+} (S = 0) in a two to one ratio [80]. In contrast, the Pr counterpart appears to have short-range order instead [81]. This results in the La material being insulating [82] in its low-temperature charge-ordered phase [80], whereas $Pr_4Ni_3O_8$ remains metallic at all temperatures [75], with an intriguing linear *T* behavior in its resistivity for intermediate temperatures (similar to that of cuprates at a comparable hole doping). Nd samples have also been studied [83], but the degree of insulating/metallic behavior seems to be sample dependent.

The difference between La and Pr trilayer materials could be due to the reduced volume associated with Pr (one of the motivations for the authors of Ref. [8] to study Sr-doped $NdNiO_2$ rather than Sr-doped $LaNiO_2$). The Ni spin state and metal versus insulator character have indeed been calculated to be sensitive to modest pressure [77]. Another factor is possible mixed valency of Pr as observed in cuprates (though Pr-M edge data on $Pr_4Ni_3O_8$ did not indicate mixed valent behavior [75]). Because of its decreased charge-transfer energy relative to $n = 5$, the rare-earth derived pockets no longer occur [84] (see **Figure 2**). This lack of $\mathcal{R}$-5*d* involvement is confirmed by the Hall coefficient that stays positive at all temperatures [44], (it remains to be understood why the thermopower in the case of $La_4Ni_3O_8$ is always negative [82], also seen in the metallic phase). In addition, these trilayer nickelates show a reduced charge-transfer energy (~ 3.5 eV as obtained from a Wannier analysis [73]) that, along with the larger effective doping level, is consistent with the strong oxygen K edge pre-peak seen in x-ray absorption data [75]. Oxygen K edge RIXS data indicate a significant contribution of oxygen 2*p* states to the doped holes [85]. As the effective hole doping level is 1/3, these materials are outside the range where superconductivity would be expected (see **Figure 1**). Reaching the desired doping range for superconductivity might be possible via electron doping. This could be achieved by replacing the rare earth with a 4 + ion (such as Ce,Th, or Zr) [86], intercalating with lithium, or gating the material with an ionic liquid.

If superconductivity were to occur, one might hope for a higher T_c as has indeed been predicted via $t - J$ model calculations [87]. Recent RIXS measurements [81], though, and find a superexchange value for $n = 3$ nearly the same as that reported for the infinite-layer material. This suggests the possibility that T_c in the whole nickelate family may be confined to relatively low temperatures compared to the cuprates. The similar value of the superexchange for $n = \infty$ and $n = 3$ is somewhat of a puzzle. Though their t_{pd} hoppings are very similar, the difference in the charge-transfer energy should have resulted in a larger superexchange for $n = 3$. The fact that it is not larger is one of the intriguing questions to be resolved in these low valence layered nickelates.

2.4 The $n = 2$ Material

The $n = 2$ member of the series, $La_3Ni_2O_6$, has been synthesized and studied as well [5, 88]. In terms of filling, it lies further away from optimal *d*-filling, being nominally $Ni^{1.5+}$: $d^{8.5}$. Experimentally, it is a semiconductor with no trace of a transition occurring at any temperature, although NMR data suggest that the AFM correlations are similar to those of the $n = 3$ material. Electronic structure studies [80] have predicted its ground state to have a charge-ordered pattern with Ni^{2+} cations in a low-spin state and the Ni^{1+}: d^9 cations forming a S = 1/2 checkerboard pattern. This charge-ordering between S = 1/2 Ni^{1+}: d^9 and non-magnetic Ni^{2+}: d^8 cations is similar to the situation in the $n = 3$ material [80]. Calculations suggest that it is quite general in these layered nickelates that the Ni^{2+} cations in this square-planar environment are non-magnetic. This has been shown by *ab* initio calculations to be the case also with the Ni^{2+} dopants in the $\mathcal{R}NiO_2$ materials [53].

2.5 The $n = 1$ Case

The long-known $\mathcal{R}_2NiO_4$ materials, with the $n = 1$ formula as above, contain Ni ions with octahedral coordination. We instead consider $Ba_2NiO_2(AgSe)_2$ (BNOAS) [89], as it represents the extreme opposite of the $n = \infty$ member, not only in regards to its d^8 valence, but also because its square planar coordination with long Ni-O bond is thought to promote "high-spin" (magnetic) behavior, that is, one hole in $d_{x^2-y^2}$, and one hole in d_{z^2}. Unlike the other n cases, the charge balanced formula is $(BaAg_2Se_2)^0(BaNiO_2)^0$; both blocking and active layers are formally neutral. BNOAS is insulating, distinguished by a magnetic susceptibiliy that is constant, thus non-magnetic, above and below a peak at T* ~130 K. This increase from and subsequent decrease to its high-T value reflects some kind of magnetic reconstruction at T* that was initially discussed in terms of canting of high-spin moments. That interpretation does not account for the constant susceptibility above and below the peak.

Valence counting indicates Ni^{2+}: d^8, so a half-filled e_g manifold. Conventional expectations are either 1) both $3d$ holes are in the $d_{x^2-y^2}$ orbital–a magnetically dead singlet that cannot account for the behavior around T*, or 2) a Hund's rule $S = 1$ triplet, which would show a Curie-Weiss susceptibility above the ordering temperature, but that is not seen in experiment. Correlated DFT calculations [90] predict an unusual Ni d^8 singlet: a singly occupied d_{z^2} orbital anti-aligned with a $d_{x^2-y^2}$ spin. This "off-diagonal singlet" consists of two fully spin-polarized $3d$ orbitals singlet-coupled, giving rise to a "non-magnetic" ion, however one having an internal orbital texture. Such tendencies were earlier noted [51] in $LaNiO_2$, and related Ni spin states were observed to be sensitive to modest pressure in the $n = 2$ and $n = 3$ classes [77]. Attempts are underway [91, 92] to understand this "magnetic transition in a non-magnetic insulator".

3 OUTLOOK

While this new nickelate family seems to be emerging as its own class of superconductors, its connections to cuprates (crystal and electronic structures, formal d count in the superconducting region, and AFM correlations) retain a focus on similarities between the two classes. Apart from the obvious structural analogy, the cuprate-motivated prediction of optimal $d^{8.8}$ filling has been realized in two nickelate materials, one achieved through chemical doping, and the other by layering dimensionality. In this context, the (so far) little studied $n = 6$ and $n = 4$ members of the series [73] may provide some prospect for superconductivity. Oxygen-reduced samples of these materials are so far lacking (though the $n = 4$ member of the RP series has been epitaxially grown [93]), and even if they are synthesized, they might require additional chemical tuning to achieve superconductivity. They share a similar electronic structure to the $n = 5$ material, but with slightly different nominal filling of the $3d$ bands [73]. Calculations show that as n decreases from $n = \infty$ to $n = 3$, the cuprate-like character increases, with the charge-transfer energy decreasing along with the self-doping effect from the rare earth $5d$ states. In contrast, the particular $n = 1$ member discussed above seems distinct from other nickelates, and provides a different set of questions in the context of quantum materials [91, 92].

AUTHOR CONTRIBUTIONS

All authors listed have made a substantial, direct, and intellectual contribution to the work and approved it for publication.

FUNDING

AB was supported by the United States National Science Foundation, Grant No. DMR 2045826. K-WL was supported by the National Research Foundation of Korea, and Grant No. NRF2019R1A2C1009588. MN was supported by the Materials Sciences and Engineering Division, Basic Energy Sciences, Office of Science, United States Department of Energy. VP acknowledges support from the MINECO of Spain through the project PGC2018-101 334-BC21. WP acknowledges support from United States National Science Foundation, Grant No. DMR 1607139.

REFERENCES

1. Greenblatt M. Ruddlesden-Popper $Ln_{n+1}Ni_nO_{3n+1}$ Nickelates: Structure and Properties. *Curr Opin Solid State Mater Sci* (1997) 2:174–83. doi:10.1016/s1359-0286(97)80062-9
2. Hayward MA, Green MA, Rosseinsky MJ, Sloan J. Sodium Hydride as a Powerful Reducing Agent for Topotactic Oxide Deintercalation: Synthesis and Characterization of the Nickel(I) Oxide $LaNiO_2$. *J Am Chem Soc* (1999) 121: 8843–54. doi:10.1021/ja991573i
3. Crespin M, Levitz P, Gatineau L. Reduced Forms of $LaNiO_3$ perovskite. Part 1.-Evidence for New Phases: $La_2Ni_2O_5$ and $LaNiO_2$. *J Chem Soc Faraday Trans 2* (1983) 79:1181–94. doi:10.1039/f29837901181
4. Crespin M, Isnard O, Dubois F, Choisnet J, Odier P. $LaNiO_2$: Synthesis and Structural Characterization. *J Solid State Chem* (2005) 178:1326–34. doi:10.1016/j.jssc.2005.01.023
5. Poltavets VV, Lokshin KA, Dikmen S, Croft M, Egami T, Greenblatt M. $La_3Ni_2O_6$: A New Double T'-type Nickelate with Infinite $Ni^{1+/2+}O_2$ Layers. *J Am Chem Soc* (2006) 128:9050–1. doi:10.1021/ja063031o
6. Kawai M, Matsumoto K, Ichikawa N, Mizumaki M, Sakata O, Kawamura N, et al. Orientation Change of an Infinite-Layer Structure $LaNiO_2$ Epitaxial Thin Film by Annealing with CaH_2. *Cryst Growth Des* (2010) 10:2044–6. doi:10.1021/cg100178y
7. Ikeda A, Manabe T, Naito M. Improved Conductivity of Infinite-Layer $LaNiO_2$ Thin Films by Metal Organic Decomposition. *Physica C: Superconductivity* (2013) 495:134–40. doi:10.1016/j.physc.2013.09.007
8. Li D, Lee K, Wang BY, Osada M, Crossley S, Lee HR, et al. Superconductivity in an Infinite-Layer Nickelate. *Nature* (2019) 572:624–7. doi:10.1038/s41586-019-1496-5
9. Zeng SW, Li CJ, Chow LE, Cao Y, Zhang ZT, Tang CS, et al. Superconductivity In Infinite-Layer Lanthanide Nickelates. *arXiv:2105.13492* (2021).
10. Osada M, Wang BY, Goodge BH, Harvey SP, Lee K, Li D, et al. Nickelate Superconductivity without Rare-Earth Magnetism: $(La,Sr)NiO_2$. *Adv Mater* (2021) 33:2104083. doi:10.1002/adma.202104083
11. Osada M, Wang BY, Goodge BH, Lee K, Yoon H, Sakuma K, et al. A Superconducting Praseodymium Nickelate with Infinite Layer Structure. *Nano Lett* (2020) 20:5735–40. doi:10.1021/acs.nanolett.0c01392

12. Li D, Wang BY, Lee K, Harvey SP, Osada M, Goodge BH, et al. Superconducting Dome in $Nd_{1-x}Sr_xNiO_2$ Infinite Layer Films. *Phys Rev Lett* (2020) 125:027001. doi:10.1103/physrevlett.125.027001
13. Zeng S, Tang CS, Yin X, Li C, Li M, Huang Z, et al. Phase Diagram and Superconducting Dome of Infinite-Layer $Nd_{1-x}Sr_xNiO_2$ Thin Films. *Phys Rev Lett* (2020) 125:147003. doi:10.1103/physrevlett.125.147003
14. Norman MR. Entering the Nickel Age of Superconductivity. *Physics* (2020) 13: 85. doi:10.1103/physics.13.85
15. Pickett WE. The Dawn of the Nickel Age of Superconductivity. *Nat Rev Phys* (2021) 3:7–8. doi:10.1038/s42254-020-00257-3
16. Lee K, Goodge BH, Li D, Osada M, Wang BY, Cui Y, et al. Aspects of the Synthesis of Thin Film Superconducting Infinite-Layer Nickelates. *APL Mater* (2020) 8:041107. doi:10.1063/5.0005103
17. Goodge BH, Li D, Lee K, Osada M, Wang BY, Sawatzky GA, et al. Doping Evolution of the Mott-Hubbard Landscape in Infinite-Layer Nickelates. *Proc Natl Acad Sci USA* (2021) 118:e2007683118. doi:10.1073/pnas.2007683118
18. Hepting M, Li D, Jia CJ, Lu H, Paris E, Tseng Y, et al. Electronic Structure of the Parent Compound of Superconducting Infinite-Layer Nickelates. *Nat Mater* (2020) 19:381–5. doi:10.1038/s41563-019-0585-z
19. Fu Y, Wang L, Cheng H, Pei S, Zhou X, Chen J, et al. Core-Level X-Ray Photoemission And Raman Spectroscopy Studies On Electronic Structures In Mott-Hubbard Type Nickelate Oxide $NdNiO_2$. *arXiv:1911.03177* (2019).
20. Li Q, He C, Si J, Zhu X, Zhang Y, Wen H-H. Absence of Superconductivity in Bulk $Nd_{1-x}Sr_xNiO_2$. *Commun Mater* (2020) 1:16. doi:10.1038/s43246-020-0018-1
21. Wang B-X, Zheng H, Krivyakina E, Chmaissem O, Lopes PP, Lynn JW, et al. Synthesis and characterization of bulk $Nd_{1-x}Sr_xNiO_2$ and $Nd_{1-x}Sr_xNiO_3$. *Phys Rev Mater* (2020) 4:084409. doi:10.1103/physrevmaterials.4.084409
22. Gu Q, Li Y, Wan S, Li H, Guo W, Yang H, et al. Single Particle Tunneling Spectrum of Superconducting $Nd_{1-x}Sr_xNiO_2$ Thin Films. *Nat Commun* (2020) 11:6027. doi:10.1038/s41467-020-19908-1
23. Jiang P, Si L, Liao Z, Zhong Z. Electronic Structure of Rare-Earth Infinite-Layer $RNiO_2$(R=La,Nd). *Phys Rev B* (2019) 100:201106. doi:10.1103/physrevb.100.201106
24. Liu Z, Ren Z, Zhu W, Wang Z, Yang J. Electronic and Magnetic Structure of Infinite-Layer $NdNiO_2$: Trace of Antiferromagnetic Metal. *Npj Quan Mater.* (2020) 5:31. doi:10.1038/s41535-020-0229-1
25. Nomura Y, Hirayama M, Tadano T, Yoshimoto Y, Nakamura K, Arita R. Formation of a Two-Dimensional Single-Component Correlated Electron System and Band Engineering in the Nickelate Superconductor $NdNiO_2$. *Phys Rev B* (2019) 100:205138. doi:10.1103/physrevb.100.205138
26. Wu X, Di Sante D, Schwemmer T, Hanke W, Hwang HY, Raghu S, et al. Robust $d_{x^2-y^2}$-wave Superconductivity Of Infinite-Layer Nickelates. *Phys Rev B* (2020) 101:060504. doi:10.1103/physrevb.101.060504
27. Choi M-Y, Lee K-W, Pickett WE. Role of 4f States in Infinite-Layer $NdNiO_2$. *Phys Rev B* (2020) 101:020503. doi:10.1103/physrevb.101.020503
28. Ryee S, Yoon H, Kim TJ, Jeong MY, Han MJ. Induced Magnetic Two-Dimensionality By Hole Doping In The Superconducting Infinite-Layer Nickelate $Nd_{1-x}Sr_xNiO_2$. *Phys Rev B* (2020) 101:064513. doi:10.1103/physrevb.101.064513
29. Gu Y, Zhu S, Wang X, Hu J, Chen H. A Substantial Hybridization between Correlated Ni-D Orbital and Itinerant Electrons in Infinite-Layer Nickelates. *Commun Phys* (2020) 3:84. doi:10.1038/s42005-020-0347-x
30. Leonov I, Skornyakov SL, Savrasov SY. Lifshitz Transition and Frustration of Magnetic Moments in Infinite-Layer $NdNiO_2$ upon Hole Doping. *Phys Rev B* (2020) 101:241108. doi:10.1103/physrevb.101.241108
31. Lechermann F. Late Transition Metal Oxides with Infinite-Layer Structure: Nickelates versus Cuprates. *Phys Rev B* (2020) 101:081110. doi:10.1103/physrevb.101.081110
32. Lechermann F. Multiorbital Processes Rule the $Nd_{1-x}Sr_xNiO_2$ normal State. *Phys Rev X* (2020) 10:041002. doi:10.1103/physrevx.10.041002
33. Hu Y, Liu G, Hao W, Liu Y, Liu Z. Experimental Study on Regression Model of Ultraviolet Laser Processing Thermal Barrier Coating Based on Response Surface Method. *J Phys Conf Ser* (2019) 1187:032046. doi:10.1088/1742-6596/1187/3/032046
34. Sakakibara H, Usui H, Suzuki K, Kotani T, Aoki H, Kuroki K. Model Construction and a Possibility of Cupratelike Pairing in a New d^9 Nickelate Superconductor (Nd, Sr)NiO_2. *Phys Rev Lett* (2020) 125:077003. doi:10.1103/physrevlett.125.077003
35. Jiang M, Berciu M, Sawatzky GA. Critical Nature of the Ni Spin State in Doped $NdNiO_2$. *Phys Rev Lett* (2020) 124:207004. doi:10.1103/physrevlett.124.207004
36. Werner P, Hoshino S. Nickelate Superconductors: Multiorbital Nature and Spin Freezing. *Phys Rev B* (2020) 101:041104. doi:10.1103/physrevb.101.041104
37. Zhang H, Jin L, Wang S, Xi B, Shi X, Ye F, et al. Effective Hamiltonian for Nickelate Oxides $Nd_{1-x}Sr_xNiO_2$. *Phys Rev Res* (2020) 2:013214. doi:10.1103/physrevresearch.2.013214
38. Karp J, Botana AS, Norman MR, Park H, Zingl M, Millis A. Many-Body Electronic Structure of $NdNiO_2$ and $CaCuO_2$. *Phys Rev X* (2020) 10:021061. doi:10.1103/physrevx.10.021061
39. Botana AS, Norman MR. Similarities and Differences between $LaNiO_2$ and $CaCuO_2$ and Implications for Superconductivity. *Phys Rev X* (2020) 10:011024. doi:10.1103/physrevx.10.011024
40. Wang Y, Kang C-J, Miao H, Kotliar G. Hund's Metal Physics: From $SrNiO_2$ to $LaNiO_2$. *Phys Rev B* (2020) 102:161118. doi:10.1103/physrevb.102.161118
41. Olevano V, Bernardini F, Blase X, Cano A. Ab Initio many-body GW Correlations in the Electronic Structure of $LaNiO_2$. *Phys Rev B* (2020) 101: 161102(R). doi:10.1103/physrevb.101.161102
42. Zhang Y-H, Vishwanath A. Type-II t-J model in Superconducting Nickelate $Nd_{1-x}Sr_xNiO_2$. *Phys Rev Res* (2020) 2:023112. doi:10.1103/physrevresearch.2.023112
43. Petocchi F, Christiansson V, Nilsson F, Aryasetiawan F, Werner P. Normal State of $Nd_{1-x}Sr_xNiO_2$ from Self-Consistent GW+EDMFT. *Phys Rev X* (2020) 10:041047. doi:10.1103/physrevx.10.041047
44. Pan GA, Segedin DF, LaBollita H, Song Q, Nica EM, Goodge BH, et al. Superconductivity in a Quintuple-layer Square-planar Nickelate. *Nat Mater (published online)* (2021). doi:10.1038/s41563-021-01142-9
45. Zhang J, Tao X. Review on quasi-2D Square Planar Nickelates. *CrystEngComm* (2021) 23:3249–64. doi:10.1039/d0ce01880e
46. Nomura Y, Arita R. Superconductivity In Infinite-Layer Nickelates. *arXiv: 2107.12923* (2021).
47. Gu Q, Wen H-H. Superconductivity In Nickel Based 112 Systems. *arXiv: 2109.07654* (2021).
48. Botana AS, Bernardini F, Cano A. Nickelate Superconductors: An Ongoing Dialog between Theory and Experiments. *J Exp Theor Phys* (2021) 132:618–27. doi:10.1134/s1063776121040026
49. Osada M, Wang BY, Lee K, Li D, Hwang HY. Phase Diagram of Infinite Layer Praseodymium Nickelate $Pr_{1-x}Sr_xNiO_2$ Thin Films. *Phys Rev Mater* (2020) 4: 121801. doi:10.1103/physrevmaterials.4.121801
50. Lu H, Rossi M, Nag A, Osada M, Li DF, Lee K, et al. Magnetic Excitations in Infinite-Layer Nickelates. *Science* (2021) 373:213–6. doi:10.1126/science.abd7726
51. Lee K-W, Pickett WE. Infinite-layer $LaNiO_2$: Ni^{1+} is not Cu^{2+}. *Phys Rev B* (2004) 70:165109. doi:10.1103/physrevb.70.165109
52. Anisimov VI, Bukhvalov D, Rice TM. Electronic Structure of Possible Nickelate Analogs to the Cuprates. *Phys Rev B* (1999) 59:7901–6. doi:10.1103/physrevb.59.7901
53. Krishna J, LaBollita H, Fumega AO, Pardo V, Botana AS. Effects of Sr Doping on the Electronic and Spin-State Properties of Infinite-Layer Nickelates: Nature of Holes. *Phys Rev B* (2020) 102:224506. doi:10.1103/physrevb.102.224506
54. Weber C, Yee C, Haule K, Kotliar G. Scaling of the Transition Temperature of Hole-Doped Cuprate Superconductors with the Charge-Transfer Energy. *Epl* (2012) 100:37001. doi:10.1209/0295-5075/100/37001
55. Been E, Lee WS, Hwang HY, Cui Y, Zaanen J, Deveraux T, et al. Electronic Structure Trends Across the Rare-Earth Series in Superconducting Infinite-Layer Nickelates. *Phys Rev X* (2021) 11:011050. doi:10.1103/physrevx.11.011050
56. Higashi K, Winder M, Kunes J, Hariki A. Core-Level X-Ray Spectroscopy of Infinite-Layer Nickelate: LDA + DMFT Study. *Phys Rev X* (2021) 11:041009. doi:10.1103/physrevx.11.041009
57. Kang B, Melnick C, Semon P, Ryee S, Han MJ, Kotliar G, et al. Infinite-Layer Nickelates As Ni-e_g Hund's Metals *arXiv:2007.14610* (2021).
58. Ryee S, Han MJ, Choi S. Hund Physics Landscape of Two-Orbital Systems. *Phys Rev Lett* (2021) 126:206401. doi:10.1103/physrevlett.126.206401

59. Liu Z, Xu C, Cao C, Zhu W, Wang ZF, Yang J. Doping Dependence of Electronic Structure of Infinite-layer $NdNiO_2$. *Phys Rev B* (2021) 103:045103. doi:10.1103/physrevb.103.045103
60. Kang C-J, Kotliar G. Optical Properties of the Infinite-Layer $La_{1-x}Sr_xNiO_2$ and Hidden Hund's Physics. *Phys Rev Lett* (2021) 126:127401. doi:10.1103/physrevlett.126.127401
61. Plienbumrung T, Daghofer M, Oleś AM. Interplay between Zhang-Rice Singlets and High-Spin States in a Model for Doped NiO_2 Planes. *Phys Rev B* (2021) 103:104513. doi:10.1103/physrevb.103.104513
62. Zhao D, Zhou YB, Fu Y, Wang L, Zhou XF, Cheng H, et al. Intrinsic Spin Susceptibility and Pseudogaplike Behavior in Infinite-Layer $LaNiO_2$. *Phys Rev Lett* (2021) 126:197001. doi:10.1103/physrevlett.126.197001
63. Lin H, Gawryluk DJ, Klein YM, Huangfu S, Pomjakushina E, von Rohr F, et al. Universal Spin-Glass Behaviour In Bulk $LaNiO_2$, $PrNiO_2$, and $NdNiO_2$. *arXiv: 2104.14324* (2021).
64. Zhang R, Lane C, Singh B, Nokelainen J, Barbiellini B, Markiewicz RS, et al. Magnetic and F-Electron Effects in $LaNiO_2$ and $NdNiO_2$ Nickelates with Cuprate-like $3d_{x^2-y^2}$ Band. *Commun Phys* (2021) 4:118. doi:10.1038/s42005-021-00621-4
65. Choi M-Y, Pickett WE, Lee K-W. Fluctuation-frustrated Flat Band Instabilities in $NdNiO_2$. *Phys Rev Res* (2020) 2:033445. doi:10.1103/physrevresearch.2.033445
66. Wu X, Di Sante D, Schwemmer T, Hanke W, Hwang HY, Raghu S, et al. Robust $d_{x^2-y^2}$ -wave Superconductivity of Infinite-layer Nickelates. *Phys Rev B* (2020) 101:060504. doi:10.1103/physrevb.101.060504
67. Gu Q, Li Y, Wan S, Li H, Guo W, Yang H, et al. Single Particle Tunneling Spectrum of Superconducting $Nd_{1-x}Sr_xNiO_2$ Thin Films. *Nat Commun* (2020) 11:6027. doi:10.1038/s41467-020-19908-1
68. He R, Jiang P, Lu Y, Song Y, Chen M, Jin M, et al. Polarity-Induced Electronic and Atomic Reconstruction at $NdNiO_2/SrTiO_3$ Interfaces. *Phys Rev B* (2020) 102:035118. doi:10.1103/physrevb.102.035118
69. Bernardini F, Cano A. Stability and Electronic Properties of $LaNiO_2/SrTiO_3$ Heterostructures. *J Phys Mater* (2020) 3:03LT01. doi:10.1088/2515-7639/ab9d0f
70. Geisler B, Pentcheva R. Correlated Interface Electron gas in Infinite-Layer Nickelate Versus Cuprate Films on $SrTiO_3$(001). *Phys Rev Res* (2021) 3:013261. doi:10.1103/physrevresearch.3.013261
71. Ortiz RA, Menke H, Misják F, Mantadakis DT, Fürsich K, Schierle E, et al. Superlattice Approach to Doping Infinite-Layer Nickelates. *Phys Rev B* (2021) 104:165137. doi:10.1103/physrevb.104.165137
72. Ren X, Gao Q, Zhao Y, Hailan Luo XZ, Zhu Z. Superconductivity in Infinite-Layer $Pr_{\{0.8\}}Sr_{\{0.2\}}NiO_2$ Films on Different Substrates. *arXiv:2109.05761* (2021).
73. LaBollita H, Botana AS. Tuning the Van Hove Singularities in AV_3Sb_5 (A=K, Rb, Cs) via Pressure and Doping. *Phys Rev B* (2021) 104:035148. doi:10.1103/physrevb.104.205129
74. Poltavets VV, Lokshin KA, Croft M, Mandal TK, Egami T, Greenblatt M. Crystal Structures of $Ln_4Ni_3O_8$ (Ln = La, Nd) Triple Layer T'-type Nickelates. *Inorg Chem* (2007) 46:10887–91. doi:10.1021/ic701480v
75. Zhang J, Botana AS, Freeland JW, Phelan D, Zheng H, Pardo V, et al. Large Orbital Polarization in a Metallic Square-Planar Nickelate. *Nat Phys* (2017) 13: 864–9. doi:10.1038/nphys4149
76. Zhang J, Chen Y-S, Phelan D, Zheng H, Norman MR, Mitchell JF. Stacked Charge Stripes in the quasi-2D Trilayer Nickelate $La_4Ni_3O_8$. *Proc Natl Acad Sci USA* (2016) 113:8945–50. doi:10.1073/pnas.1606637113
77. Pardo V, Pickett WE. Pressure-Induced Metal-Insulator and Spin-State Transition in Low-Valence Layered Nickelates. *Phys Rev B* (2012) 85:045111. doi:10.1103/physrevb.85.045111
78. Karp J, Hampel A, Zingl M, Botana AS, Park H, Norman MR, et al. Comparative many-body Study of $Pr_4Ni_3O_8$ and $NdNiO_2$. *Phys Rev B* (2020) 102:245130. doi:10.1103/physrevb.102.245130
79. Zhang J, Pajerowski DM, Botana AS, Zheng H, Harriger L, Rodriguez-Rivera J, et al. Spin Stripe Order in a Square Planar Trilayer Nickelate. *Phys Rev Lett* (2019) 122:247201. doi:10.1103/physrevlett.122.247201
80. Botana AS, Pardo V, Pickett WE, Norman MR. Charge Ordering in Ni^{1+}/Ni^{2+} Nickelates: $La_4Ni_3O_8$ and $La_3Ni_2O_6$. *Phys Rev B* (2016) 94:081105. doi:10.1103/physrevb.94.081105
81. Lin JQ, Villar Arribi P, Fabbris G, Botana AS, Meyers D, Miao H, et al. Strong Superexchange in a $d^{9-\delta}$ Nickelate Revealed by Resonant Inelastic X-Ray Scattering. *Phys Rev Lett* (2021) 126:087001. doi:10.1103/physrevlett.126.087001
82. Cheng J-G, Zhou J-S, Goodenough JB, Zhou HD, Matsubayashi K, Uwatoko Y, et al. Pressure Effect on the Structural Transition and Suppression of the High-Spin State in the Triple-LayerT'–$La_4Ni_3O_8$. *Phys Rev Lett* (2012) 108:236403. doi:10.1103/physrevlett.108.236403
83. Retoux R, Rodriguez-Carvajal J, Lacorre P. Neutron Diffraction and TEM Studies of the Crystal Structure and Defects of $Nd_4Ni_3O_8$. *J Solid State Chem* (1998) 140:307–15. doi:10.1006/jssc.1998.7892
84. Pardo V, Pickett WE. Quantum Confinement Induced Molecular Correlated Insulating State in $La_4Ni_3O_8$. *Phys Rev Lett* (2010) 105:266402. doi:10.1103/physrevlett.105.266402
85. Shen Y, Sears J, Fabbris G, Li J, Pelliciari J, Jarrige I, et al. Role of Oxygen States in Square Planar d^9-Delta Nickelates. *arXiv:2110.08937* (2021).
86. Botana AS, Pardo V, Norman MR. Electron Doped Layered Nickelates: Spanning the Phase Diagram of the Cuprates. *Phys Rev Mater* (2017) 1: 021801. doi:10.1103/physrevmaterials.1.021801
87. Nica EM, Krishna J, Yu R, Si Q, Botana AS, Erten O. Theoretical Investigation of Superconductivity in Trilayer Square-Planar Nickelates. *Phys Rev B* (2020) 102:020504. doi:10.1103/physrevb.102.020504
88. Crocker J, Dioguardi A, Shirer K, Poltavets V, Greenblatt M, Klavins P, et al. NMR Evidence for Spin Fluctuations in the Bilayer Nickelate $La_3Ni_2O_6$. *Phys Rev B* (2013) 88:075124.
89. Matsumoto Y, Yamamoto T, Nakano K, Takatsu H, Murakami T, Hongo K, et al. High-Pressure Synthesis of $A_2NiO_2Ag_2Se_2$ (A=Sr, Ba) with a High-Spin Ni^{2+} in Square-Planar Coordination. *Angew Chem Int Ed* (2019) 58:756–9. doi:10.1002/anie.201810161
90. Jin H-S, Pickett WE, Lee K-W. Proposed Ordering of Textured Spin Singlets in a Bulk Infinite-Layer Nickelate. *Phys Rev Res* (2020) 2:033197. doi:10.1103/physrevresearch.2.033197
91. Tu W-L, Moon E-G, Lee K-W, Pickett WE, Lee H-Y Field-Induced Bose-Einstein Condensation and Supersolid in the Two-Dimensional Kondo Necklace. *arXiv:2107.11936* (2021).
92. Singh RRP Magnetism of Competing High-Spin/Low-Spin States in $Ba_2NiO_2(AgSe)_2$ and Related Two-Orbital Two-Electron Systems. *arXiv: 2108.09706* (2021).
93. Li Z, Guo W, Zhang TT, Song JH, Gao TY, Gu ZB, et al. Epitaxial Growth and Electronic Structure of Ruddlesden-Popper Nickelates ($Ln_{n+1}Ni_nO_{3n+1}$, n = 1-5). *APL Mater* (2020) 8:091112. doi:10.1063/5.0018934

Conflict of Interest: The authors declare that the research was conducted in the absence of any commercial or financial relationships that could be construed as a potential conflict of interest.

Publisher's Note: All claims expressed in this article are solely those of the authors and do not necessarily represent those of their affiliated organizations, or those of the publisher, the editors and the reviewers. Any product that may be evaluated in this article, or claim that may be made by its manufacturer, is not guaranteed or endorsed by the publisher.